Interpretation of small-angle x-ray scattering data from dilute montmorillonite suspensions using a modified Guinier approximation

C. Shang and J. A. Rice*
Department of Chemistry and Biochemistry, South Dakota State University, Brookings, South Dakota 57007-0896
(Received 17 January 2001; published 18 July 2001)

Smectites are a group of 2:1-layer phyllosilicate minerals that have been extensively studied by small-angle x-ray scattering (SAXS) because of their industrial and environmental significance. In previous studies, a Guinier plot has been used to obtain the radius of gyration of the clay particles, from which geometric information of the particle structure is derived. Using an indirect Fourier transform to treat SAXS data from a dilute montmorillonite suspension, a negative electron contrast at the clay-water interface is observed. This electron inhomogeneity has violated the assumption underlying the application of the Guinier plot, which requires particles to have a uniform electron density. The presence of this inhomogeneity explains the inability of previous studies to correctly determine particle dimensions using the Guinier plot. Using this model of the clay-water interface, a modified Guinier plot has been derived and was experimentally verified. The calculation shows the presence of negative electron contrast at montmorillonite-water interfaces, which is in accordance with the results from the indirect Fourier transform method. This approximation has the potential to predict the geometric information for similar colloids studied by small-angle scattering.

DOI: 10.1103/PhysRevE.64.021401 PACS number(s): 83.80.Hj

I. INTRODUCTION

Montmorillonite belongs to a group of 2:1-layer silicates known as smectites that are common in soils and sediments [1]. Because of the charge deficit in its crystal lattice and small particle size under natural conditions, the surface properties and colloidal behavior of these clay minerals have been studied using various techniques [2]. Small-angle x-ray scattering (SAXS), which is capable of revealing internal and surface structures over length scales from approximately 0.5 to 1000 nm [3,4], has been used to characterize these minerals in suspension and in the gel phase [5–11].

The intensity $I(q)$ of scattered x rays of wavelength λ as a function of the scattering vector q for randomly oriented scatterers with a continuous charge distribution can be stated as [3]

$$I(q)=\int_V\int_V \rho(\mathbf{r}_1)\rho(\mathbf{r}_2)[\sin(qr_{12})/(qr_{12})]dV_1dV_2, \quad (1)$$

where $q=(4\pi/\lambda)\sin(\theta/2)$ with θ being the scattering angle, V is the particle volume, $\rho(\mathbf{r})$ is a continuous electron distribution with position $\mathbf{r}$, and $r_{12}=|\mathbf{r}_1-\mathbf{r}_2|$ [3]. For an isotropic distribution of N_p particles of a particular shape that take all orientations with equal probability, an exact solution for $I(q)$ can be obtained [12]:

$$I(q)=N_p(V\rho)^2 i(q). \quad (2)$$

For a flat disk of infinitesimal thickness and diameter $2R$,

$$i(q)=[2/(qR)^2][1-J_1(2qR)/(qR)], \quad (3)$$

where $J_1(x)$ is the Bessel function of first kind and order one.

At small q, Guinier's approximation of $I(q)$ in Eq. (1) can be obtained. If the origins of the coordinate systems for integration over V_1 and V_2 are taken at the center of charge of the scatterer, and with $\sin(qr)/(qr)=1-(qr)^2/6+\cdots$,

$$I(q)=N_p\langle[V\rho(\mathbf{r})]^2\rangle[1-(qR_g)^2+\cdots] \quad (4)$$

with

$$R_g^2=V\left(\int_V \rho(\mathbf{r})r^2dV\right)\Big/\left(\int_V \rho(\mathbf{r})dV\right), \quad (5)$$

where "$\langle\ \rangle$" represents an average [3]. For a thin disk of diameter $2R$ and thickness T [12],

$$I(q)\approx N_p(V\rho)^2 2\exp(-q^2R_g^2)/(qR)^2, \quad (6)$$

where R_g is the radius of gyration of a scatterer with reference to the particle's electron density distribution and $R_g^2=T^2/12$. The radius of gyration can be obtained from either Eq. (5) or more conveniently by a plot of $\ln[I(q)]$ vs q^2 using Eq. (6) (a so-called "Guinier plot"). The use of a Guinier plot to derive geometric dimensions of a particle requires that two conditions be satisfied, that the particles scatter independently of each other and that particles have a uniform electron density [13].

According to Eq. (6), a plot of $\ln[I(q)q^2]$ vs q^2 is a straight line for thin-layer particle systems like montmorillonite. The radius of gyration, and thus the thickness of particle, can be derived from the slope of this plot. This plot has two important applications. It reveals whether the unknown particles are thin layer in shape by inspecting the plot's linearity, and if the plot is a linear at small q, the thickness of the particle can be obtained.

*Author to whom correspondence should be addressed. FAX: 605-688-6364. Email address: james_rice@sdstate.edu

However, there are discrepancies in the literature on the application of this technique to determine the thickness of smectite particles or pseudocrystals. Thompson and Butterworth [14] reported that the Guinier plot of SAXS data from a 2% Na-laponite suspension (a synthetic smectite) gave a particle thickness of 3.9 nm rather than 0.92 nm (the single layer thickness). A similar value (3.4–3.5 nm) was found by Saunders *et al.* [11] for two different preparations of Li-laponite that was dispersed in water at 0.03% w/w, *p*H 10 and ionic strength of $10^{-3}\,\mathrm{mol\,L^{-1}}$. These authors interpreted their thickness values as indicative of the presence of two to three clay platelets separated by adsorbed water layers [11,14]. Using small-angle neutron scattering, Cebula *et al.* [15] found that the radius of gyration of a Li-montmorillonite dispersed in water corresponded to a plate thickness of 3.5 nm. They determined the thickness of clay pseudocrystals by varying the neutron-density contrast between the suspending medium and the particles. There are experimental difficulties that make these interpretations of particle thickness less than convincing. In all the cases, the clay concentrations were close to, or lower than the critical concentration corresponding to the covolume of clay suspension (the volume around the particle from which a second particle is excluded) [17]. This means that some of the suspensions studied in these reports contained essentially independent particles, an observation that is particularly applicable to the samples of Saunders *et al.* [11], who adjusted the suspension *p*H to 10. At most, there existed a certain degree of covolume overlapping in their samples, but not an interlayer structure. The choice of experimental conditions should have eliminated the possibility of multiparticle stacking. And if a structure with two- or three-layer stacking was present in those systems, a Bragg reflection should have been observed, but this was not the case [11,14,15].

We believe that we now have an explanation for why a Guinier plot failed to give an accurate account of the particle thickness in independent particle systems. Shang *et al.* [18] used an indirect Fourier transform method to treat SAXS results from dilute montmorillonite suspensions (0.5–2% w/w), and showed that a negative electron contrast exists at the particle-solution interface using the scattering length density profile of scatterers. We believe that the presence of an electron inhomogeneity in the scatterers (aluminosilicate layer and interfaces) invalidates the use of the Guinier approximation applied in previously cited or similar studies. In this paper we present a modified Guinier approximation taking into account the electron distribution inhomogeneity of the scattering particles based on our results obtained from the indirect Fourier transform of the scattering data. We will demonstrate the agreement between the results from the modified Guinier plot and from the indirect Fourier transform data, and the potential of the modified plot for future use.

II. EXPERIMENT

Montmorillonite (SWy-2) was obtained from the Source Clay Minerals Repository, University of Missouri-Columbia, Missouri. The mineral has a unit cell dimension of $a=5.17\,\text{Å}\times b=8.95\,\text{Å}$, a chemical composition of $Na_{0.76}(Al_{3.06}Fe_{0.30}Fe_{0.02}Mg_{0.65})(Al_{0.18}Si_{7.82})O_{20}(OH)_4$, cation exchange capacity $102\,\mathrm{cmol_c\,kg^{-1}}$ and specific surface area of $750\,\mathrm{m^2\,g^{-1}}$ [2,19,20]. The clay sample was first treated with *p*H=5 acetate buffer to remove carbonates, hydrogen peroxide (30%) to oxidize organic matter, and dithionite in citrate-bicarbonate buffer to remove free iron oxides [18]. The treated clay was shaken with 1*M* NaCl for 6 h before centrifugation and the supernatant discarded. The salt washing was repeated once. The Na-saturated clay was washed once with distilled-deionized water, and dialyzed against distilled-deionized water until a silver nitrate test was negative. The <0.08-μm Na-montmorillonite fraction was obtained by centrifugation (IEC, CRU-5000). Dilute clay suspensions were concentrated on a rotary evaporator to produce a 3% w/w clay stock suspension from which three dilute suspensions (0.5%, 1.0%, and 2%) were prepared. The exact clay concentrations were determined by oven-drying a known volume and weight of clay suspension at 110 °C and weighing.

The SAXS measurements were carried out on the 10-m SAXS camera at Oak Ridge National Laboratory, Oak Ridge, TN. The camera has point collimation and a two-dimensional position sensitive detector. It is described in detail by Wignall *et al.* [21]. The distance between the sample and the detector was 1.119 m for the small-q region measurements ($0.18-4.5\ \mathrm{nm^{-1}}$) and 5.119 m for the large-q region ($0.053-0.9\ \mathrm{nm^{-1}}$). Cu $K\alpha$ radiation ($\lambda=0.154\,\mathrm{nm}$) with a power setting at 40 kV and 60 mA was used. The detector sensitivity was calibrated with a Fe-55 standard. The transmission coefficient was determined, and the data for each sample were corrected for absolute intensity. Clay suspensions were mounted in a metal cell (internal thickness of 1 mm) fitted with Kapton windows. The scanning time varied from 30 to 180 min depending on sample concentrations and the scattering vector range. The scattering from pure water was used for background subtraction because the volume fraction of the scattering clay particles is very small.

After background subtraction, the experimental scattering intensity of clay samples was expressed as intensity per unit clay concentration by dividing the intensity with the appropriate clay concentration. To remove particle concentration effects, the scattering curves were extrapolated to zero concentration using a linear Zimm plot [22].

III. RESULTS AND DISCUSSION

A. SAXS data

The experimental and extrapolated SAXS curves are given in Fig. 1(a). The scattering intensity decays according to q^{-2} for a wide range of q. This is typical of scattering by thin-layer particles. Figure 1(b) shows the zero clay concentration Guinier plot for thin-layer scatterers. The linearity of the plot over the low-q range suggests that particle concentration effects were completely removed by the extrapolation; if the effects were present, the curve should abruptly decrease at low values of q^2. The calculated radius of gyration ($R_g^2=0.5292$) corresponds to a layer thickness 25.2 Å. This is equivalent to the thickness of a montmorillonite

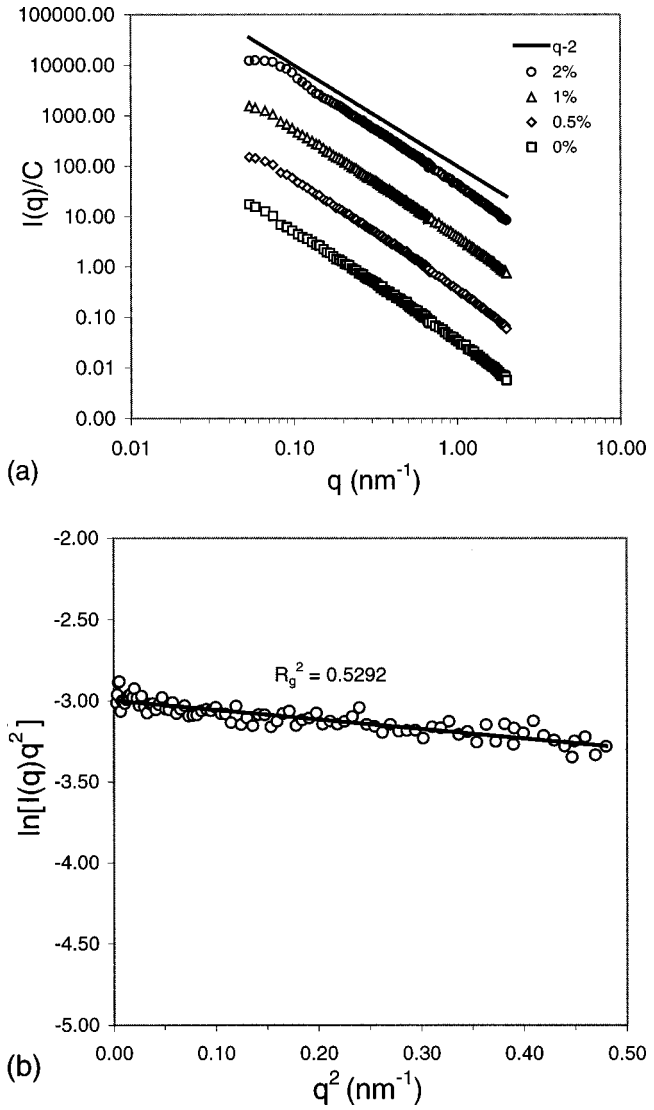

FIG. 1. Normalized and extrapolated scattering curves (a) and the Guinier plot of thickness after removing concentration effect (b) for dilution montmorillonite suspensions. The curves in (a) were arbitrarily separated by one log-cycle for presentation clarity.

pseudocrystal consisting of two platelets separated by two layers of water [23]. The particle concentration of <1 μm montmorillonite at its covolume is 4 g L^{-1} [17], and an increase in clay concentration would increase the degree of particle overlapping. In other words, free particles are expected at concentrations below the critical value if the adsorbed cations and solution composition favor the formation of a diffuse double layer (e.g., Na saturation and in water). The lowest clay concentration used in this study was 0.5%, which is close to the critical value. The Guinier plot [Fig. 1(b)] shows the elimination of the concentration effect; therefore, the apparent particle thickness derived from the Guinier plot clearly does not describe this system correctly. This argument brings our attention to the second prerequisite for using the Guinier approximation for calculating geometric dimensions, a scatterer must have a uniform electron density distribution.

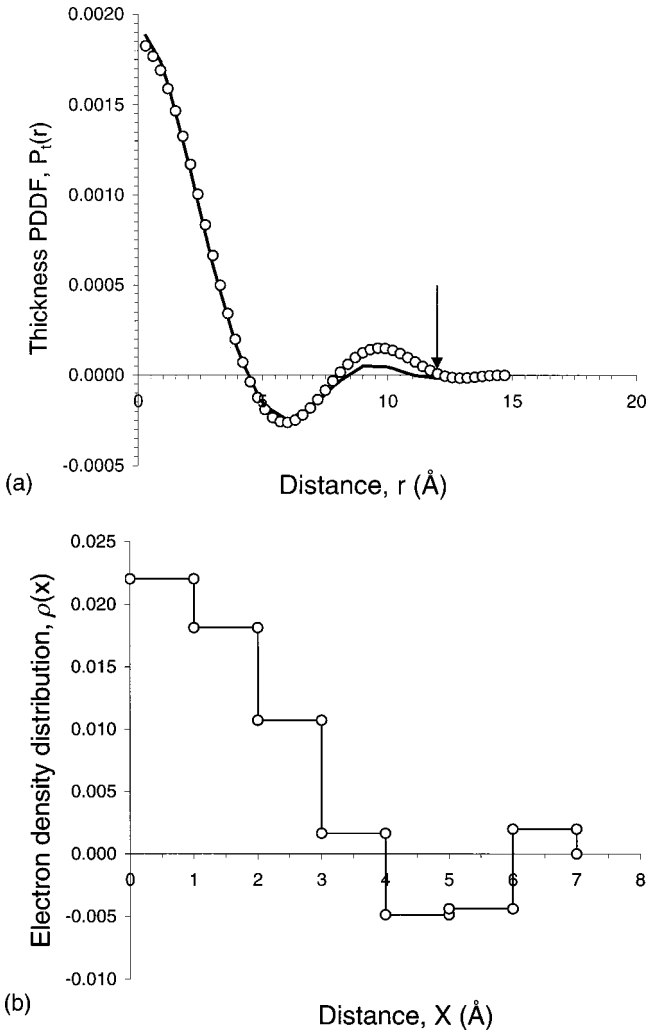

FIG. 2. The PDDF (a) and electron density contrast profile (b) obtained by the indirect Fourier transformation of the SAXS data from a 0.5% montmorillonite suspension. The solid line in (a) is the predicted PDDF using the results in (b).

B. Indirect Fourier transformation of SAXS data

The indirect Fourier transform is a numerical method developed by Glatter [24,25] to convert SAXS data in reciprocal space into geometric information about the scatterer in real space. The direct consequence of this technique is the derivation of the pair-distance-distribution function (PDDF) that contains information regarding the shape and dimension of scattering particles in the sample (PDDF$=0$, at $r \geqslant T_{\max}$, which is the maximum dimension of the scatterer). If the scatterer has central symmetry, the electron density profile, or scattering-length density profile, can be obtained from the PDDF by a deconvolution square root technique [26]. Figure 2 shows the results from analyzing the 0.5% curve using the indirect Fourier transform [18] and contains three pieces of useful information. First, the PDDF pattern [Fig. 2(a)] indicates that the scattering particle has a bilayer structure with two distinctive electron densities, a pattern that is similar to a bilayer of self-organized ionic surfactants [27]. Second, the thickness of a scattering particle is about 12 Å, thicker than 9.2 Å for a single silicate layer. Third, the electron density

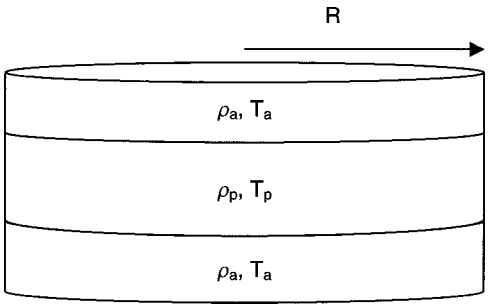

FIG. 3. Depiction of montomorillonite particles as a circular thin disk (diameter 2R) with two distinct electron densities by SAXS. ρ_a = electron density of adsorbed layer with a layer thickness T_a, ρ_p = electron density of 2:1 silicate layer of thickness T_p, and $T_t = 2T_a + T_p$.

profile [Fig. 2(b)] indicates that there is a negative electron contrast zone at the particle-water interface (i.e., a zone with an electron density lower than that of bulk water). A slightly larger scattering particle thickness can be readily explained by the presence of an adsorbed layer of water molecules and/or cations, which may alter the electron density distribution. Mourchid *et al.* [28] used Monte Carlo simulation to compute SAXS spectra for laponite samples and found that a layer thickness of 13.2 Å gave better agreement with experimental observations. This indicates that a solvated sodium counter-ion layer of 4.0 Å has to be taken into account. Based on the results discussed above, we depict the structure of a montmorillonite scatterer in suspension as a single clay layer sandwiched between two adsorbed layers with different electron densities (Fig. 3).

C. Modified Guinier approximation

When a scatterer of electron density ρ_p is suspended in a medium of electron density ρ_m the scattering intensity can be obtained from Eq. (2) by the ''two-phase'' approximation [3],

$$I(q) = N_p (V\Delta\rho)^2 i(q), \tag{7}$$

where $\Delta\rho = \rho_p - \rho_m$.
Equation (7) can then be rewritten as

$$I(q) = N_p (V\Delta\rho)^2 F^2(q), \tag{8}$$

where $i(q) = F^2(q)$.
According to Guinier and Fournet [12], the scattering intensity of the scatterer shown in Fig. 3 can be given by

$$I(q) = N_p [(\rho_a - \rho_m) V_t F_t + (\rho_p - \rho_a) V_p F_p]^2, \tag{9}$$

where V is the volume and the subscripts t and p represent total and particle, respectively. It is worth noting that formulation of Hanley *et al.* [29] for a similar system is incorrect. The authors treated the ''$F(q)$'' term as form factor, which is $F^2(q)$. For a contrast variation experiment, where adjusting the medium's electron density for $\rho_a = \rho_m$, Eq. (9) can be reduced to Eqs. (7) or (8).

Since $V = TA$, Eq. (9) can be rewritten as

$$I(q) = N_p A^2 [(\rho_a - \rho_m) T_1 F_t + (\rho_p - \rho_a) T_p F_p]^2. \tag{10}$$

where T is the particle thickness and A the particle-base surface area. Setting $\Delta\rho_a = \rho_a - \rho_m$ and $\Delta\rho_p = \rho_p - \rho_a$, and expanding, Eq. (10) becomes

$$I(q) = N_p A^2 (\Delta\rho_a^2 T_t^2 F_t^2 + \Delta\rho_p^2 T_p^2 F_p^2 + 2\Delta\rho_a \Delta\rho_p T_t T_p F_t F_p). \tag{11}$$

The F^2 terms are obtained directly from the Guinier approximation in Eq. (6), but there is no mathematical expression for the $F_t F_p$ term because of the sign problem. Here we introduce a physical approximation. Because $F_t F_p$ represents intensity, then $F_t F_p \geqslant 0$. Thus $F_t^2 \geqslant F_t F_p \geqslant F_p^2$. Thus, we can use the expression of Eq. (6) having a thickness T, where $T_t \geqslant T \geqslant T_p$, to approximate $F_t F_p$. With this approximation and rearrangement, Eq. (11) becomes

$$I(q) q^2 = \frac{2N_p A^2}{R^2 (\Delta\rho_a^2 T_t^2 + \Delta\rho_p^2 T_p^2 + 2\Delta\rho_a \Delta\rho_p T_t T_p)} \exp\left[-\frac{q^2}{12} \left(\frac{\Delta\rho_a^2 T_t^4 + \Delta\rho_p^2 T_p^4 + 2\Delta\rho_a \Delta\rho_p T_t T_p T^2}{\Delta\rho_a^2 T_t^2 + \Delta\rho_p^2 T_p^2 + 2\Delta\rho_a \Delta\rho_p T_t T_p} \right) \right]. \tag{12}$$

The slope of a plot of $\ln[I(q)q^2]$ vs q^2 from Eq. (12) is the radius of gyration and equals

$$R_g^2 = \frac{1}{12} \frac{\Delta\rho_a^2 T_t^4 + \Delta\rho_p^2 T_p^4 + 2\Delta\rho_a \Delta\rho_p T_t T_p T^2}{\Delta\rho_a^2 T_t^2 + \Delta\rho_p^2 T_p^2 + 2\Delta\rho_a \Delta\rho_p T_t T_p}. \tag{13}$$

By comparison to Eq. (6), it can be seen that Eq. (12) is the Guinier approximation modified to accommodate a scatterer with an inhomogeneous electron density distribution (as depicted in Fig. 3). For particles with a homogeneous electron density distribution (i.e., $\Delta\rho_a = 0$), Eq. (12) is reduced to Eq. (6).

In the right-hand side of Eq. (13), ρ_p, ρ_m, T_t, T_p are known, or can be safely assumed. If a value of T is given, then ρ_a can be obtained from the experimental determined R_g^2 value obtained from Fig. 1(b). We calculated $\rho_m = 0.3334\ \mathrm{e/Å^3}$ (electron density of water at room temperature) and $\rho_p = 0.8544\ \mathrm{e/Å^3}$ (electron density of montmorillonite anion), and chose $T_p = 9.2$ Å, $T_t = 14.2$ Å assuming 2.5 Å hydration layer (see Fig. 3), and $T = 11.7$ Å (average of T_p and T_t). When the calculated R_g^2 [the right-hand side of Eq. (13)] is plotted against a set of hypothetical values for ρ_a (Fig. 4), the ρ_a value corresponding to the experimental R_g^2 [Fig. 1(b)] can be obtained by linear regression.

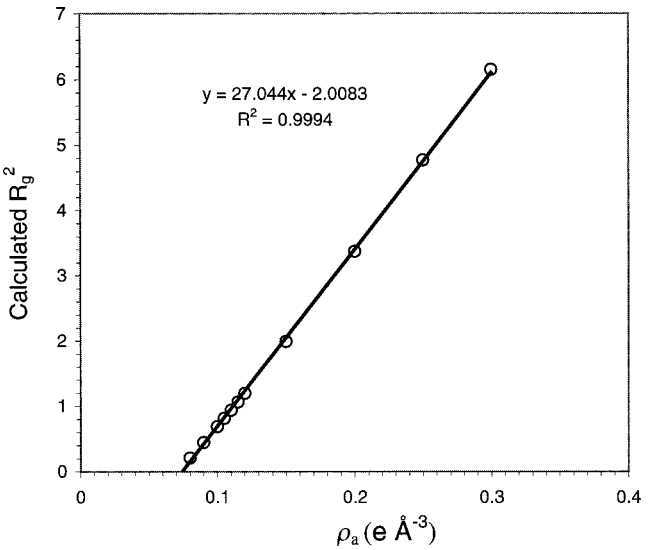

FIG. 4. A plot of calculated R_g^2 [the right-hand side of Eq. (13)] vs ρ_a.

The effect of T on the calculated ρ_a was examined over the range of values between T_p and T_t. The calculated radius of gyration is a linear function of ρ_a and converges on the experimental R_g^2 when T is equal to or greater than 11.7 Å, the average of T_p and T_t (Fig. 4). However, the relationship becomes a polynomial and does not converge to the experimental value when T is smaller than 11.7 Å (not shown).

The calculated ρ_a values, and the number of water molecules per unit charge and unit cell within the first hydration layer ($T_t = 14.2$ Å) for various values of T are given in Table I. Also given are the values for $T_t(11.7\ \text{Å})$ from Fig. 2(a). For $T_t = 14.5$ Å, these values are presented with the assumption that sodium cations are located within the first hydration layer. The number of water molecules per unit charge would increase by one if we assume that sodium cations are dissociated from the first hydration layer, which is probable [30,31]. The results show that the electron density at these interfaces is lower than that of normal liquid water, and it decreases as the distance to the mineral surface decreases (Table I).

Although the results are qualitative because the resolution of the SAXS measurements are limited by the x-ray wavelength and the approximations involved in the calculation, they are in good agreement with what has been shown by the indirect Fourier transform analysis shown in Fig. 2: there is a negative electron contrast at the montmorillonite particle-water interface. This, in turn, supports our hypothesis that in dilute dispersions, montmorillonite particles have electron density distributions that dictate that they should be treated as inhomogeneous scatterers as depicted in Fig. 3. We believe it is this electron density perturbation at the interface that leads to the erroneous results discussed previously when the Guinier approximation in the form of Eq. (6) is used on scattering data. The Guinier approximation does not yield the dimensions of montmorillonitelike particles and should be modified to account for the inhomogeneity in the electron density distribution as we have done in Eq. (12). Contradictory to the reports discussed earlier and the results presented above, the Guinier plot [in the form of Eq. (6)] for a dilute Na-laponite suspension (0.025 g mL^{-1}) by Avery and Ramsay [16] indicated a circular, disk-like clay particle having a 1.0 nm thickness. However, their results were graphically presented on an arbitrary scale and thus cannot be numerically reexamined here.

A lower electron density at the interface of the montmorillonite-water system suggests that the density (g cm^{-3}) of adsorbed water is lower than that of liquid water although the structural interpretation of a reduced water density is not conclusive [32]. The density of adsorbed water was reported to be lower than that of liquid water, decreasing to approximately that of ice at 10 Å from the surface of montmorillonite (the same clay used in this study) [33]. Martin [32] concluded that the density of water adsorbed on Na montmorillonite has a minimum value of about 0.97 g cm^{-3} at a water content of 0.7 g H_2O per gram of clay, increases rapidly to 1.4 g cm^{-3} for water content less than 0.7, and rises gradually until at 6.5 g H_2O per gram of clay the density of adsorbed water equals that of normal liquid water. It

TABLE I. The calculated ρ_a and the number of water molecules per unit charge or per unit cell for two total thickness values (T_t). Over the chosen range of T, ρ_a is always smaller than that of the zero electron-density contrast.

$T_t = 14.5$ Å				$T_t = 11.7$ Å			
T (Å)	ρ_a (e/Å^3)	H_2O/c[a]	H_2O/cell	T (Å)	ρ_a (e/Å^3)	H_2O/c[a]	H_2O/cell
11.7	0.1333	3.3	1.2	11.0	0.0274	0.44	0.16
12.0	0.1532	3.9	1.4	11.2	0.0673	1.08	0.39
12.5	0.1884	5.1	1.8	11.4	0.0921	1.48	0.53
13.0	0.2139	5.9	2.1	11.6	0.1130	1.82	0.65
13.6	0.2325	6.5	2.3	11.7	0.1219	1.96	0.71
14.2	0.2456	6.9	2.5				
Zero contrast	0.3334	10.0	3.9				

[a]The number of water molecules per unit charge if assuming Na^+ suited within the first hydration layer; this number would increase by one if assuming Na^+ is not included in the layer.

should be pointed out that the data reviewed by Martin [32] were obtained by a variety of thermodynamic methods that might not possess the sensitivity to determine the difference in density between the adsorbed and bulk water at high water contents.

The modified Guinier approximation presented here [Eqs. (12) and (13)] can potentially be used to derive the structural parameters of a scatterer having two distinctive electron densities if the densities are known. An example of such a scatterer is the geochemical organomineral composite known as ''humin'' [34]. Such scatterers were also demonstrated in laboratory studies [29,35,36].

IV. CONCLUSION

A modified Guinier equation that takes into account the inhomogeneity of the electron density distribution of a scatterer has provided an explanation for the discrepancy between the theoretical particle size of montmorillonite particles in dilute suspensions and the experimental particle sizes obtained from SAXS measurements analyzed by the classical Guinier method. This has been confirmed by application of an indirect Fourier transform of the SAXS data that demonstrates that as a scatterer, montmorillonite has an electron density at the particle-water interface lower than that of liquid water. The equations derived [Eqs. (12) and (13)] could be used to find the dimensions of similar scatterers.

ACKNOWLEDGMENTS

The project was supported by a grant from the USDA National Research Initiative Competitive Grants program through Award No. 98-35107-6515. Use of the SAXS facility was sponsored in part by the U.S. Department of Energy under Contract No. DE-AC05-00OR22725 with the Oak Ridge National Laboratory, managed by the UT-Battelle, LLC. We thank Dr. J. S. Lin for his help in providing access to the 10-m SAXS facility at ORNL.

[1] G. Borchardt, in *Minerals in Soil Environments*, edited by J. B. Dixon and S. B. Weed (Soil Science Society of America, Madison, 1989).
[2] H. van Olphen, *An Introduction to Clay Colloid Chemistry*, 2nd ed. (Wiley, New York, 1977).
[3] P. W. Schmidt, in *Modern Aspects of Small-Angle Scattering*, edited by H. Brumberger (Kluwer Academic, Dordercht, 1995).
[4] P. W. Schmidt, F. Ehrburger-Dolle, P. Pfeifer, T. Rieker, Y. M. Kapoor, and D. J. Voss, in *Disordered Materials and Interfaces*, edited by H. E. Stanley *et al.*, Mater. Res. Soc. Symp. Proc. No. **407**, (Materials Research Society Pittsburgh, 1996).
[5] R. J. Jr. Hight, W. T. Higdon, and P. W. Schmidt, J. Chem. Phys. **33**, 1656 (1960).
[6] R. J. Hight, Jr., W. T. Higdon, H. C. Darley, and P. W. Schmidt, J. Chem. Phys. **37**, 502 (1962).
[7] T. R. Taylor and P. W. Schmidt, Clays Clay Miner. **17**, 77 (1969).
[8] C. H. Pons, F. Rousseaux, and D. Tchoubar, Clay Miner. **16**, 23 (1981).
[9] M. Morvan, D. Espinat, J. Lambard, and Th. Zemb, Colloids Surf., A **82**, 193 (1994).
[10] F. Pignon, A. Magnin, J. M. Piau, B. Cabane, P. Lindner, and O. Diat, Phys. Rev. E **56**, 3281 (1997).
[11] J. M. Saunders, J. W. Goodwin, R. M. Richardson, and B. Vincent, J. Phys. Chem. B **103**, 9211 (1999).
[12] A. Guinier and G. Fournet, *Small Angle Scattering of X-rays* (Wiley, New York, 1955); J. S. Pedersen, Adv. Colloid Interface Sci. **70**, 171 (1997).
[13] G. Porod, in *Small Angle X-ray Scattering*, edited by O. Glatter and O. Kratky (Academic London, 1982).
[14] D. W. Thompson and J. T. Butterworth, J. Colloid Interface Sci. **151**, 236 (1992).
[15] D. J. Cebula, R. K. Thomas, and J. W. White, J. Chem. Soc., Faraday Trans. 1 **76**, 314 (1980).
[16] R. G. Avery and J. F. D. Ramsay, J. Colloid Interface Sci. **109**, 448 (1986).
[17] M. B. McBride, in *Minerals in Soil Environments*, 2nd ed. in Ref. [1].
[18] C. Shang, J. A. Rice, and J. S. Lin, Clays Clay Miner. (2001) (to be published).
[19] D. M. C. MacEwan, in *The X-ray Identification and Crystal structures of Clay Minerals*, 2nd ed., edited by G. Brown (Mineralogical Society, London, 1961).
[20] L. G. Schultz, Clays Clay Miner. **17**, 115 (1969).
[21] G. D. Wignall, J. S. Lin, and S. Spooner, J. Appl. Crystallogr. **23**, 241 (1990).
[22] I. Pilz, in *Small Angle X-ray Scattering*, edited by O. Glatter and O. Kratky (Academic, London, 1982).
[23] R. W. Mooney, A. C. Keenan, and L. A. Wood, J. Am. Chem. Soc. **74**, 1367 (1952).
[24] O. Glatter, J. Appl. Crystallogr. **10**, 415 (1977).
[25] O. Glatter, J. Appl. Crystallogr. **13**, 577 (1980).
[26] O. Glatter, J. Appl. Crystallogr. **12**, 166 (1979).
[27] D. J. Iampietro, L. L. Brasher, E. W. Kaler, A. Stradner, and O. Glatter, J. Phys. Chem. B **102**, 3105 (1998).
[28] A. Mourchid, A. Delville, and P. Levitz, Faraday Discuss. **101**, 275 (1995).
[29] H. J. M. Hanley, C. D. Muzny, and B. D. Butler, Langmuir **13**, 5276 (1997).
[30] N. T. Skipper, G. Sposito, F. R. C. Chang, Clays Clay Miner. **43**, 294 (1995).
[31] G. Sposito and R. Prost, Chem. Rev. **82**, 553 (1982).
[32] R. T. Martin, Clays Clay Miner. **9**, 28 (1962).
[33] D. M. Anderson and P. F. Low, Soil Sci. Soc. Am. Proc. **22**, 99 (1958).
[34] J. A. Rice and P. MacCarthy, Environ. Sci. Technol. **24**, 1875 (1990).
[35] I. Marković, R. H. Ottewill, D. J. Cebula, I. Field, and J. F. Marsh, Colloid Polym. Sci. **262**, 648 (1986).
[36] I. Grillo, P. Levitz, and Th. Zemb, Eur. Phys. J. B **10**, 29 (1999).